Phase contrast X-ray imaging

Article *in* International Journal of Nanotechnology · January 2006

DOI: 10.1504/IJNT.2006.009584 · Source: OAI

4 authors, including:

Byung Mook Weon
Sungkyunkwan University
127 PUBLICATIONS **1,128** CITATIONS
SEE PROFILE

J. H. Je
Pohang University of Science and Technology
414 PUBLICATIONS **5,473** CITATIONS
SEE PROFILE

G. Margaritondo
École Polytechnique Fédérale de Lausanne
1,059 PUBLICATIONS **17,224** CITATIONS
SEE PROFILE

Phase contrast X-ray imaging

Byung Mook Weon

Biomedical Imaging Center,
Department of Materials Science and Engineering,
Pohang University of Science and Technology,
Pohang, 790-784, Korea
E-mail: bmweon@postech.ac.kr

Jung Ho Je*

Biomedical Imaging Center, I-BIO Program,
Department of Materials Science and Engineering,
Pohang University of Science and Technology,
Pohang, 790-784, Korea
E-mail: jhje@postech.ac.kr
*Corresponding author

Yeukuang Hwu

Institute of Physics,
Academia Sinica, Nankang, Taipei 11529, Taiwan
E-mail: phhwu@sinica.edu.tw

Giorgio Margaritondo

Institut de Physique des Nanostructures,
Ecole Polytechnique Fédérale de Lausanne,
1015, Lausanne, Switzerland
E-mail: giorgio.margaritondo@epfl.ch

Abstract: In the last decade X-ray imaging based on phase contrast greatly advanced thanks to the use of unmonochromatic synchrotron hard X-rays. The recent advances are going beyond microradiology and microtomography to reach nanometre scale. This paper reviews basic theory and selected applications to biomedical and materials sciences. The forthcoming improvements in phase contrast X-ray imaging will lead to even better imaging of many different phenomena at nanometre level.

Keywords: X-ray imaging; phase contrast; hard X-ray; unmonochromatic beam; microradiology; microtomography; nanoradiology.

Reference to this paper should be made as follows: Weon, B.M., Je, J.H., Hwu, Y. and Margaritondo, G. (2006) 'Phase contrast X-ray imaging', *Int. J. Nanotechnology*, Vol. 3, Nos. 2/3, pp.280–297.

Biographical notes: Byung Mook Weon, who studied Materials Science at Pohang University of Science and Technology (POSTECH), is currently focusing on complex dynamics of physical and biological systems using synchrotron X-ray imaging through Biomedical Imaging Center as a PhD candidate of Department of Materials Science and Engineering in POSTECH.

Jung Ho Je, who obtained his PhD Degree in Materials Science at Korea Advanced Institute of Science and Technology (KAIST) in 1983, is a Professor of Department of Materials Science and Engineering and I-Bio Program, and a director of Biomedical Imaging Center in POSTECH. For two decades, he has been working on the fields of Materials Science, Physics, and recently Biophysics, especially using synchrotron X-rays. His field of expertise and research interests is nanostructural properties and X-ray imaging using synchrotron X-rays.

Yeukuang Hwu, who received his PhD Degree in Physics at University of Wisconsin-Madison in USA, is a Professor of Academia Sinica in Taiwan, on various topics of synchrotron radiation research. In recent years, his research focus has been on phase contrast X-ray imaging and its applications to physical or biological systems.

Giorgio Margaritondo, who was born at Rome in 1946, is a citizen of USA. He received Laurea (Summa Cum Laude) in Physics in University of Rome in 1969. He was a professor in University of Wisconsin-Madison between 1978 and 1990. He is a Dean, Faculty of Basic Sciences since 1990 and also the Vice-President for Academic Affairs (provost) of Ecole Polytechnique Fédérale de Lausanne (EPFL) in Switzerland. His field of expertise and research interests concerns the physics of semiconductors and superconductors (electronic states, surfaces and interfaces) and of biological systems; his main experimental techniques are electron spectroscopy and spectromicroscopy, X-ray imaging and scanning near-field microscopy, including experiments with synchrotron light and with free electron lasers.

1 Introduction

Since Röntgen's discovery of X-rays in 1895 [1], X-ray imaging with hard X-rays has been an important diagnostic tool in medicine, biology, and materials science [2]. In the last decade X-ray imaging has greatly advanced together with the improvement of synchrotron radiation sources [3,4]. Such sources provide high-resolution, non-destructive, and non-invasive imaging for microradiology and microtomography [4], which solves a major problem of detection of internal structures of live systems. Highly coherent synchrotron X-ray sources are exploited for non-conventional contrast mechanisms [5].

In particular, phase contrast X-ray imaging is a powerful technique for the detection of low contrast details in weakly absorbing materials [6,7]. The phase contrast technique is based on the observation of the interference pattern between diffracted and undiffracted waves produced by spatial variations of the real part of the refractive index [6,7]. Several research groups are exploring ways of exploiting phase effects as a source of image contrast. These approaches fall into three broad categories [5]: interferometry [8–13], diffractometry [14,15], and phase contrast radiography (or in-line holography) [16–25].

Importantly, a monochromatic beam is not necessary – spatial coherence is much more important than spectral coherence [5,16,25]. On this basis, successful applications of unmonochromatic synchrotron hard X-rays to real systems have been implemented by several groups [25–38].

This paper reviews basic theory of phase contrast X-ray imaging using unmonochromatic synchrotron hard X-rays and illustrates selected applications in biomedical and materials sciences realised in our laboratories. Future improvements in synchrotron X-ray imaging targeting high lateral resolution down to 20 nm and high time resolution down to 10 μs would play a significant role in research on both physical and biological systems with characteristic length scales in the nanometre range. The on-going progress in phase contrast X-ray imaging will enable us to visualise more clearly many different phenomena of nanoscience and nanotechnology.

2 Fundamentals

2.1 Imaging techniques

The best reference case for microradiology is the early detection of tumours [39]. Despite recent advances in cancer research techniques, biomedical scientists are still limited in their ability to detect tumours in their earliest stage of formation, monitor tumour phenotype, quantify invasion or metastasis, or visualise real-time, in vivo activity of anticancer therapeutics [39]. Techniques such as magnetic resonance imaging (MRI), X-ray computed tomography (CT), nuclear imaging, optical imaging, and ultrasound, as summarised in Table 1, are likely to revolutionise the way researchers detect and monitor cancer over the next decade [39]. For higher magnification and better resolution one usually relies on electron microscopy, which can reveal details down to a few nanometers.

Biological cell samples for electron microscopy require painstaking preparation procedures [40]. Even for optical microscopy, a tissue usually has to be fixed (that is, preserved by pickling in a reactive chemical solution), supported by embedding in a solid wax or resin, sectioned into thin slices, and stained before it is viewed. For electron microscopy similar procedures are required, but the sections must be much thinner and it is not possible to analyse living, wet cells [40].

On the contrary, X-ray microscopy is a very powerful method that can investigate whole cells in their aqueous environment avoiding potential artefacts introduced by the dehydration or fixation necessary with other techniques [41]. Since Röntgen found that X-rays can reveal bone structures [1], X-rays have been developed primarily for their use in medical imaging [2]. Radiology and radiological tomography is indeed the most common use of X-rays. X-ray imaging is especially useful in the detection of pathologies of the skeletal system, but is also widely applied for detecting many disease processes in soft tissues. Some notable examples are the common chest radiographs that reveal lung diseases such as pneumonia, lung cancer or pulmonary oedema, and the abdominal radiographs that can detect ileus (blockage of the intestine), free air (from visceral perforations) and free fluid (in ascites). In some cases the use of X-rays is more problematic, such as the detection of gallstones (which are rarely radio-opaque) or kidney stones (which are often but not always visible). Also, X-rays encounter serious difficulties in the imaging of soft tissues such as the brain or muscle. Imaging alternatives

for soft tissues are computed tomography (CT), magnetic resonance imaging (MRI), or ultrasound imaging [39]. On the other hand, X-rays can be used in 'real-time' procedures such as angiography or contrast studies of hollow organs using fluoroscopy. Angioplasty, a therapeutic procedure for the arterial system, relies on X-ray-sensitive contrast agents to identify potentially treatable lesions. Phase-contrast X-ray microscopy and microtomography are the natural continuation and enhancement of these techniques.

Table 1 Overview of biomedical imaging systems [39]

Technique	*Resolution*	*Depth*	*Time*	*Imaging agents*	*Primary use*
Magnetic resonance imaging (MRI)	10–100 μm	No limit	Min/hours	Gadolium, dysprosium, iron oxide particles	Best all-round imaging system with high contrast; used in phenotyping, physiological imaging and cell tracking
X-ray computed tomography (CT) imaging	50 μm	No limit	Min	Iodine	Lung and bone-tumour imaging
Ultrasound imaging	50 μm	mm	Min	Micro bubble	Vascular and interventional imaging
Positron emission tomography (PET) imaging	1–2 mm	No limit	Min	^{18}F, ^{11}C, ^{15}O	Imaging metabolism of molecules, such as glucose, thymidine and so on
Single photon emission tomography (SPECT) imaging	1–2 mm	No limit	Min	^{99m}Tc, ^{111}In	Imaging of probes such as antibodies, peptides and so on
Fluorescence reflectance imaging (FRI)	1–2 mm	<1 cm	Sec/Min	Fluorescent protein NIR fluorochromes	Rapid screening of molecular events in surface-based tumours
Fluorescence-mediated tomography (FMT)	1–2 mm	<10 cm	Sec/min	NIR fluorochromes	Quantitative imaging of targeted or 'smart' fluorochrome reporters in deep tumours
Bioluminescence imaging (BLI)	Several mm	Cm	Min	Luciferin	Gene expression, cell tracking
Intravital microscopy (confocal, multiphoton)	1 μm	<400 μm	Sec/min	Fluorescent protein, photoprotein, fluorochromes	All of the above at higher resolutions but at limited depths and coverage

2.2 Synchrotron X-rays

The characteristics of synchrotron X-ray sources, quite different from those of conventional sources, are exploited by several novel imaging techniques [3,31]. The different radiology approaches based on synchrotron sources are summarised in Table 2 [30].

Table 2 Summary overview of synchrotron-based radiology techniques [30]

	Synchrotron mammography	*Two-wavelength angiography (dichromography)*	*Phase contrast imaging*	*Diffraction-enhanced imaging*	*Synchrotron microtomography*
Main imaging mechanisms(s)	Absorption (phase contrast, refraction)	Absorption	Phase constant, refraction	Diffraction	Absorption, phase contrast, refraction
Wavelengths	Single	Two	Single or broadband	Single or broadband	Single or broadband
Imaged body part	Breast tissue	Coronaries and other blood vessels	Any tissue	Any tissue	Any tissue
Current applications	Phantoms, anatomical specimens	Live patients	Anatomical and biological specimens	Anatomical and biological specimens	Anatomical and biological specimens
Potential applications	Live patients	Routine examinations of live patients	Live patients	Live patients	Possibly live patients
Advantages over conventional radiology	High contrast for low dose	Peripheral venous injection of contrast agent	Very high contrast for lower dose, high lateral and time resolution	Very high contrast for lower dose, high lateral resolution, separation of absorption and non-absorption features	Very high contrast for lower dose, high lateral resolution
Problems	Not yet a certified technique for medical use	Complicated implementation	Non-conventional image features, require special interpretation techniques	Non-conventional image features, require special interpretation techniques	For phase-contrast: non-conventional image features, require special interpretation techniques
Time per image	1–10 s	Tens of milliseconds	<1 ms	Down to milliseconds	Several seconds (for complete image set)
Spatial resolution	30 μm	Hundreds of microns	Better than 1 μm	Better than 1 μm (tens of micron for possible images in vivo)	Better than 1 μm
Three-dimensional imaging	No	No	No	No	Yes

Synchrotron sources provide X-rays that are intense, vertically collimated, polarised, and continuous over a wide energy range [3,17]. Synchrotron radiation is the light emitted by electrons as they circulate around a high-energy accelerator [3]. This light covers a spectrum from hard (short wavelength) X-rays through soft (long wavelength) X-rays, ultraviolet, visible, and infrared radiation. Specifically, the synchrotron sources called undulators and wigglers provide beams collimated both in the horizontal and the vertical directions. An advanced 'wiggler' synchrotron source can beat the brightness of a conventional emitter by 12 orders of magnitude or more [31].

A synchrotron X-ray microscope uses electromagnetic radiation from a synchrotron source to image small objects thanks to the interaction between the radiation and matter. Unlike visible light, X-rays do not reflect or refract easily, and they are invisible to the human eye. Therefore the basic approach of a synchrotron X-ray microscope is to use a film or a charge-coupled device (CCD) to detect X-rays that pass through the specimen, rather than light that is reflected or diffused by the specimen. The X-ray detection for imaging applications can also be based on materials such as NaI (sodium iodide) that can 'convert' X-ray photons into visible photons, which can then be converted into an electronic signal by a photomultiplier. These detectors are called 'scintillators' [31].

2.3 Soft X-ray vs. hard X-ray

The most important advantage of X-rays is the short wavelength that leads to higher spatial resolution. X-rays are indeed electromagnetic waves with a wavelength in the range of 10 to 10^{-3} nanometers [3]. Roughly speaking, X-rays with a wavelength longer than 1 Å (corresponding to a photon energy smaller than ~12.4 keV) are called *soft X-rays*. At wavelengths shorter than 1 Å (photon energies larger than ~12.4 keV), one uses the term *hard X-rays*.

Biological cells can be effectively imaged in soft X-ray microscopy using X-rays with wavelengths in the so-called 'water window' (284 ~ 543 eV) that maximises the contrast between carbon-containing areas and water [33]. The 'water window' provides a contrast mechanism for imaging because carbon in organic materials absorbs the corresponding soft X-rays and oxygen in water is transparent to them. The development of advanced soft X-ray optics successfully achieved the observation of subcell structures in the hydrated state. However, soft X-rays in this photon energy range cannot penetrate specimens thicker than a few tens of a micrometer, approximately the thickness of a single cell, and this limits their potential applications [33]. Moreover, this type of approach was so far unable to produce images of living cells due to the sample preparation requirements [33].

Hard X-rays (>12.4 keV) have a large penetration depth and are well suited for the non-destructive investigation of thick opaque samples [42]. Furthermore, the combination of hard X-ray microscopy with tomographic reconstruction enabled us to obtain three-dimensional (3D) information on a specimen even on the submicrometer scale with minimal sample preparation [42]. In recent years, intense research efforts drastically improved the lateral resolution and enhanced the contrast in these techniques [25–33]. Most recently, it was proven that synchrotron hard X-rays are suitable for radiological imaging of thick and live biological samples down to the cellular level [33].

2.4 Unmonochromatised beams

With an unmonochromatised ('white') beam, the signal becomes very high and detailed images can be obtained on a microscopic scale [25–33]. The lateral resolution reaches submicron levels suitable for imaging individual cells and can be further improved [30,32]. White beams also make it possible to take real-time images with a time resolution that reaches the millisecond level and is also rapidly improving [30,32]. The strategy of using unmonochromatised X-ray beams derives from a detailed theoretical analysis of the conditions for phase contrast microradiology and from subsequent experimental validation of the results [25–33]. Our findings were in agreement with the results of other authors [16–18, 20–22, 43–45]. The basic conclusion was that the typical edge-enhancement mechanism that improves the image quality only requires a moderate level of time coherence, i.e., it does not require monochromatic X-rays. Without a monochromator, it is possible to avoid the related losses and increase the flux on the object by several orders of magnitude. This is the strategy that opened the door not only to high spatial resolution but also to high time resolution [25–33].

2.5 Phase contrast X-ray imaging

Phase contrast X-ray imaging was first tested by Snigirev et al. [20,21] and by David et al. [16] and Wilkins et al. [17], who obtained high-contrast and high-spatial resolution images of different organic samples [7]. The basic concept for phase contrast X-ray imaging was discussed by Hwu et al. [26,29]. The parameter used to describe the interaction of electromagnetic radiation with matter is the complex refractive index [6,7], $n = 1-\delta + i\beta$, where β is the absorption term and δ is the phase shift term. The difference in wavelength dependence between β and δ makes it possible for δ to produce detectable effects even when the absorption is negligible, since β is very small [6,7].

The real term δ describes phenomena like refraction, diffraction and interference and effects related to the phase of the X-ray waves. The imaginary part corresponds to the strength of absorption loss at a particular wavelength. Thus, the imaginary part is sometimes called the extinction coefficient. Absorption losses become particularly significant, for example, in metals at visible wavelengths. On the contrary, in a dielectric material such as glass, the visible light is not absorbed and therefore $\beta = 0$. In conventional radiology, the image contrast is entirely due to absorption and corresponds to the imaginary term β. On the contrary, effects related to the real part are typically not observable and do not contribute to contrast. In phase contrast techniques the opposite is true and such effects are predominant. At very short wavelengths (several angstroms), the real part can become larger than the imaginary part. Therefore, the advantage of phase contrast over absorption contrast becomes more significant for hard X-rays (wavelengths shorter than 1 Å) [29].

Figure 1 illustrates an example of imaging related to the real term δ; note, in particular, the characteristic effect of edge enhancement. Refraction-based edge enhancement is essentially due to the fact that different specimen regions with different δ-values produce by refraction different lateral displacements of a collimated X-ray beam [29]. The refraction at the edge region deflects the beam by an angle η, whose value depends on the edge slope and on the δ-value. Consider the average distance a between the dark and illustrated fringes on the detector, and the width of each fringe b. The distance a is determined by the width of the tapered edge; thus, it is a morphological

characteristic of the object. On the other hand, the fringe width is given by $b \approx r_0 \eta$, which increases with the object-detector distance r_0.

As a consequence, edge enhancement due to refraction is visible only for certain values of r_0. As r_0 changes, there is an interesting interplay between the refraction effect and another phenomenon related to the real term δ: edge diffraction that produces a series of fringes. As the object-detector distance r_0 is reduced, we should first observe refraction-based edge enhancement at least for some edges. Then the diffraction-based edge enhancement may become visible, whereas the refraction-based edge enhancement is reduced. Therefore, it is possible to select either the 'refraction' regime or the 'diffraction' regime by simply moving the detector. In general, the refraction-based mechanism offers advantages over the diffraction-based mechanism. The images are simpler and easier to interpret. The edge enhancement due to refraction is easier to detect even with limited detector resolution.

Figure 1 Schematic explanation of the edge enhancement by the 'refraction' mechanism [26]

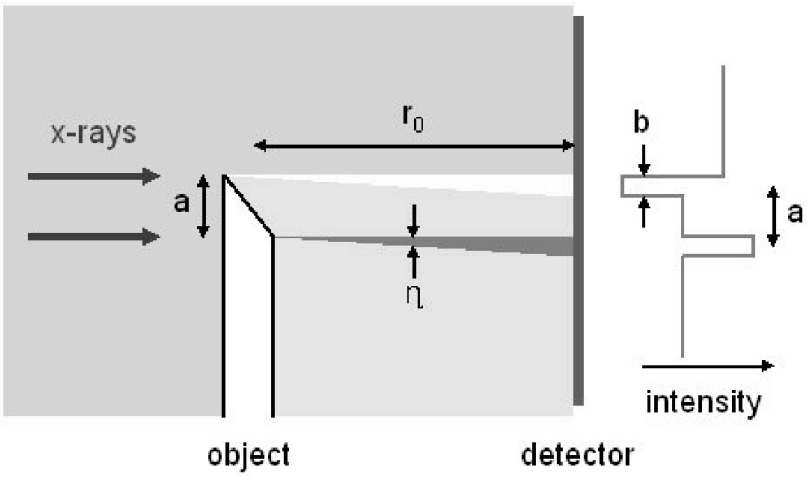

The onset of diffraction enhancement as r_0 increases can be clearly seen in the images of Figure 2, which show two crossed 30 μm diameter *W* wires for r_0 = 0.03, 0.25, 0.50, 0.70, and 1.0 m. We note that three important points:

- the diffraction fringes are not visible for the two smaller values of r_0, barely visible at r_0 = 0.50 m, clearly visible at r_0 = 0.70 m, and very clear at r_0 = 1.0 m
- without diffraction there is no edge enhancement, which is due to the strongly absorbing character of the wire that impedes the refraction enhancement
- the diffraction can be seen for the horizontal edge and not for the vertical edge.

This last effect is due to the properties of the 'bending magnet' synchrotron source used in this case; contrary to wigglers and undulators, such a source is only collimated in the vertical direction [29].

Figure 2 Sequence of radiographic images of 30 μm diameter crossed *W* wires, taken at a photon energy of 9 keV for object-detector distance (from left to right) r_0 = 0.03, 0.25, 0.50, 0.70 and 1.0 m [29]

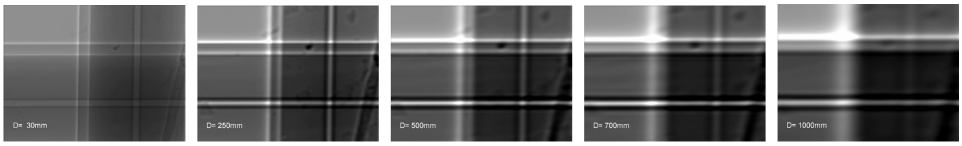

Edge enhancement by refraction or diffraction cannot be easily observed with conventional X-ray sources due to their large size and angular spread. In fact, the enhancement is due to small deviations of the X-rays propagating through the edge. A large source size and angular spread wash out the effect. To reduce this problem, one can either use an aperture to limit the effective source size or increase the source-sample distance. However, this greatly reduces the portion of the emitted X-rays that is actually used for radiological imaging. Synchrotron sources directly provide collimated beams suitable for phase-contrast techniques.

In summary, phase contrast X-ray imaging is sensitive to density and refraction gradients in the object and does not rely on absorption. Thus, it can image weakly absorbing materials, such as carbon-based materials and biological systems [16]. This raises the possibility of non-invasive clinical diagnostic imaging. It should be noted that the sensitivity of absorption contrast decrease as the photon energy increases as E^{-3}, whereas that of phase contrast methods decrease only as E^{-2} [16]. This is why phase contrast methods become more sensitive at higher energies; as a consequence, for comparable image quality the absorbed X-ray dose is smaller than with conventional radiography, minimising sample damage [16]. This raises interesting possibilities in diagnostics applications. By using white radiation and a time-resolving system, it was possible to image microscopic details of moving blood vessels in different live animals without using any contrast agent [32]. The images have excellent contrast plus unprecedented spatial resolution for microangiography. Results of this kind are likely to impact many different areas of biological and medical research and of diagnostic radiology [30].

3 Applications

3.1 Synchrotron X-ray imaging at the Pohang light source

The 7B2 beamline of the Pohang Light Source (PLS) in Korea, operated by a Korean-Taiwanese-Swiss consortium, is fully dedicated to microimaging experiment in real time with coherent X-rays [31]. The performances of the first tests already reached excellent levels when compared to other similar facilities worldwide. The key feature is the use of white or unmonochromatic X-rays to achieve very high lateral and time resolution. The total length of the beamline, 34.8 m, was selected to provide a large beam on the object.

The imaging techniques implemented on the beamline are influenced by the ratio between the source-object distance and the object-detector distance. The 34.8 m length is the maximum allowed by the PLS building and is perfectly suitable for the relevant

experiments. Figure 3 shows the schematic diagram of the end station for synchrotron X-ray imaging. The attenuator, which consists of a variable number of *Si* wafers, modifies not only the intensity but also the photon energy spectrum. The high-pass effect of the attenuator is desirable when low energy photons are not desired. The attenuator is followed by the sample positioning system and by the image detection system. The sample holder allows adjustment of three coordinates (with 0.1 μm accuracy) plus tilting and rotation. A goniometer is designed to perform rotations with an accuracy of 0.001 degree for tomography and other applications. The longitudinal coordinate can be varied over a large range corresponding to object-detector distances from 5 mm to 1.5 m. This is a very important feature for coherent X-ray imaging since – as we have seen – the detection of the edge-enhancing fringes depends on the detector resolution and on the object-detector distance. The X-ray intensity is converted into visible light by a scintillator consisting of a 150 μm thick cleaved $CdWO_4$ single crystal. The scintillator material was selected to simultaneously optimise the conversion efficiency and the scintillator contribution to the lateral resolution. The material is quite resistant to exposure to hard radiation. The image produced by the scintillator is reflected by a mirror to avoid exposure of the detection system to hard X-rays, and then magnified by an optical lens system. The lens system is interchangeable, with magnification from 1*x* to 50*x*. The magnified image is then detected by a CCD camera. Depending on the specific applications, several CCD cameras can be selected with shutter speeds ranging from 1 ms to 1 hour. The number of pixels range up to 1600 × 1200 with 14 bit grey scale.

Figure 3 The schematic diagram of the end station for synchrotron X-ray imaging

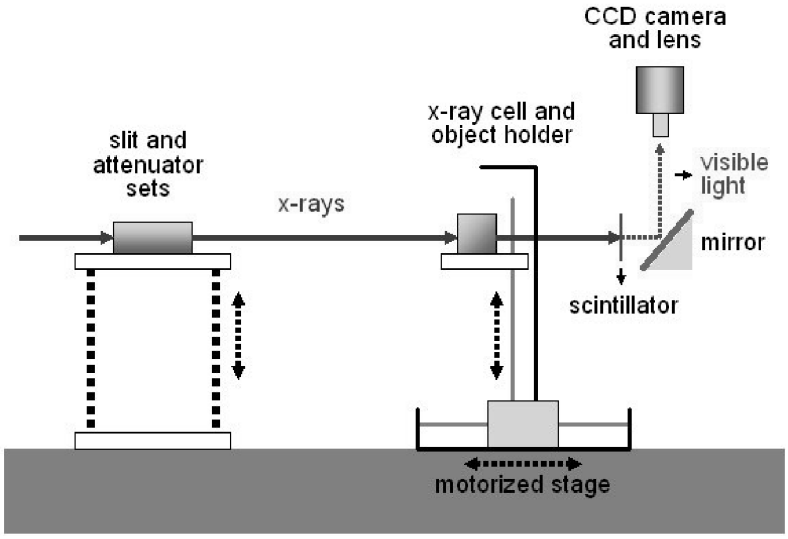

Many tests enabled us to compare the beamline performances to those of several other similar facilities at PLS (5C1 beamline), SRRC-Taiwan, Elettra-Trieste, APS-Argonne, and SSLS-Singapore. We can conclude that the present performances of the 7B2 beamline in terms of obtaining high quality phase contrast microradiographs and the measurement speed either match or in some cases surpass those of comparable facilities [31].

3.2 Biomedical sciences

As we already mentioned, by using unmonochromatised radiation and a time-resolving system it is possible to image microscopic details of moving blood vessels in different live animals without using any contrast agent [32]. The images have excellent contrast plus unprecedented spatial resolution for microangiography (<10 μm). Figure 4 shows typical examples of microangiography images. Figures 4(a) and 4(b) show tortuous draining vessels of a rat eyeball, with faintly visible intermingled vasculatures indicative of the choroidal vascular plexus. Note that in the case of Figure 4(a), a small amount of iodine contrast dye with half dilution was injected before taking the image through a pre-inserted polyethylene tube into the common carotid artery of the same side. This image provided a reference to show that the imaged microfeatures without contrast agent are indeed blood vessels in motion.

Figure 4 Microangiographs of the eye and auricle regions in live rats [33]. Prior to image taking, a contrast dye was injected through the proximal common carotid artery at the anterior neck with a fine polyethylene tube inserted for about 5 mm towards the head before the carotid bifurcation site. (a) and (b) are eye angiograms taken during (a) and several minutes after (b) the passage of the dye. (c) and (d) are auricle angiograms, taken during (d1) or after (c and d2) the passage of the dye. The exposure time of each photo was 15 ms

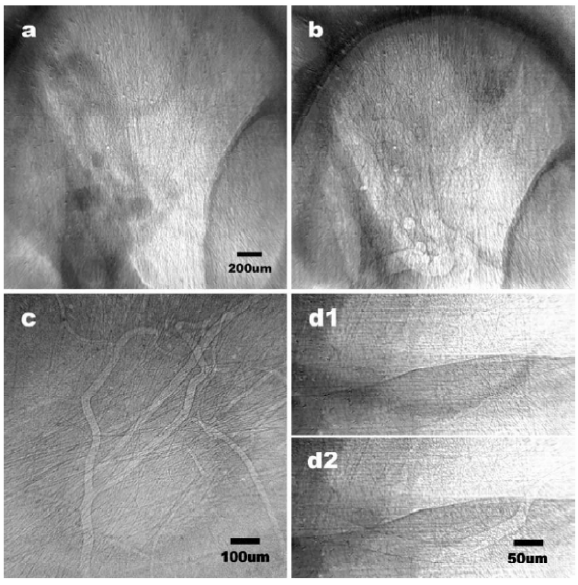

Can individual cells, including live cells, be imaged using hard X-rays? Common wisdom until now required sophisticated staining techniques for this task. Most recently, Hwu et al. showed that individual cells and cell details can be detected in culture solution and tissues with no staining and no other contrast-enhancing preparation [33]. The sample examined can be much thicker than for many other microscopy techniques without sacrificing the capability to resolve individual cells. The first successful tests were conducted on a variety of cell systems including skin and internal leaf cells, mouse neurons, rabbit fibroblast cells, and human tumour cells [33].

Phase-contrast radiological cell imaging is an interesting complementary approach to the standard optical microscopy of living cells. In fact, X-ray microradiology has the capability to examine thicker samples in a more 'realistic' environment and potentially even in living bodies. Hwu et al. demonstrated, for example, that cellular detail within a sample as thick as 5 mm can still be clearly identified at a selected depth from the sample surface without sacrificing the lateral resolution. Furthermore, recent tests based on advances in detectors and in image reconstruction demonstrated that the short wavelength of hard X-rays can yield reconstructed images with 10 ~ 50 nm resolution well beyond the diffraction limit of optical microscopy [45].

To clearly demonstrate this high 'selectivity' resulting from the enhanced contrast due to phase effect and from the high-penetration nature of X-rays, the local tomography reconstruction of a toothpick is shown in Figure 5(a). The diameter of the toothpick is 3 mm and the reconstructed area is 240×240 μm. Figure 5(b) shows the 3D volume-rendered surface contour image constructed from the tomography reconstructed data as examples in Figure 5(a). Note that not only each channel but also the texture of the cell walls along the direction parallel to the rotation axis are clearly imaged. Likewise, using refractive index radiology, fine details can be indeed imaged with high lateral and time resolution in a variety of biology materials [33]. These include leaf skin cells, human tumour cells, mouse neurons, and rabbit bone cells.

Figure 5 (a) Tomographic reconstruction of a toothpick, used to assess the resolution performances of apparatus and procedure. The diameter of the sample is 3 mm but only a central area of diameter 240 μm is reconstructed. Features of μm size can be observed and (b) the volume-rendered 3D structure of the same toothpick sample [33]

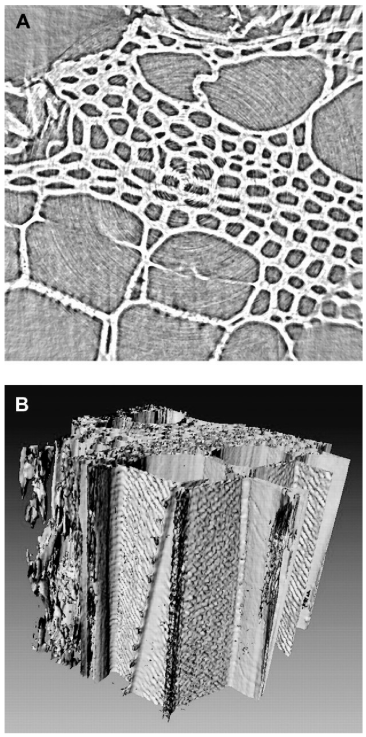

With suitable fixation procedures, Hwu et al. could even obtain high-resolution microtomography and 3D reconstructed images of mammalian cells [33]. The sample examined was a piece of aorta fixed in resin; the overall sample dimension, including the resin, is $5 \times 7 \times 10$ mm. Figure 6 is the volume-rendered 3D structure of this sample. The white arrows point to borders between neighbouring cells, whereas the black arrow points to a cell nucleus that extrudes from the surface and whose outline is well presented in the 3D reconstruction analysis [33]. In this case, the imaging capability goes beyond the mere imaging of the outline and shape of the individual cell and provides subcell information [33]. Figure 7 demonstrates the volume-rendered 3D tomographic view of an aloe leaf sample, which shows the stoma area with clear view of individual cells. Images are regenerated for front (a) and (b) or rear skin (c) and (d).

Figure 6 The volume-rendered 3D structure of an aorta sample [33]. The white arrows point to borders between neighboring cells, whereas the black arrow points a cell nucleus that extrudes from the surface and whose outline is well preserved in the 3D reconstruction. Scale bar is 5 μm

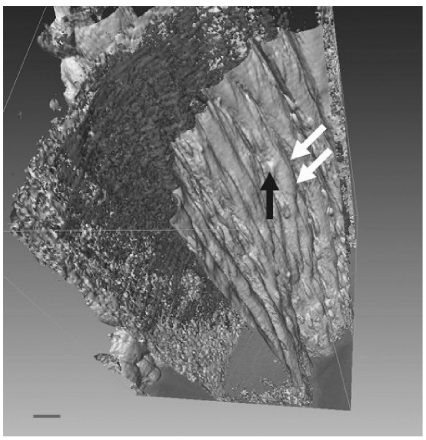

Figure 7 The volume-rendered 3D tomographic view of an aloe leaf sample. This shows the stoma area with clear view of individual cells. Images are regenerated for front (a) and (b) or rear skin (c) and (d)

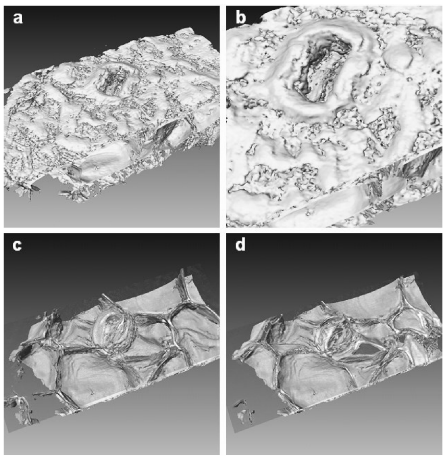

3.3 Materials sciences

Time and lateral resolution also play a very important role in non-biological applications of radiology [28,32,34,46,47]. Microradiology movies, for example, can solve long-standing issues in materials science phenomena by direct real-time observation. Figure 8 shows an excellent example: the direct detection of an almost incredible phenomenon in the electrodeposition of thin metal coating. As clearly seen in the radiology movie frames, the electrodeposition process creates hydrogen bubbles at the substrate-coating interface. The metal coating grows on the fast-developing bubbles. This eventually leads to the formation of spherical voids that finally explain a common kind of coating defects. In another interesting study, phase contrast radiology using unmonochromatic synchrotron X-ray successfully imaged the grain boundaries of Al and AlZn alloy without contrast agent [34]. Combining the high penetration of X-ray and the 3D reconstruction by microtomography, they were able to nondestructively characterise the polycrystalline materials [34].

Figure 8 Real-time edge-enhanced microradiology applied to materials science [30]. The two frames captured from a radiology movie reveal a very surprising phenomenon during a metal coating procedure: the metal growths on gas bubbles forming on the substrate during the deposition process

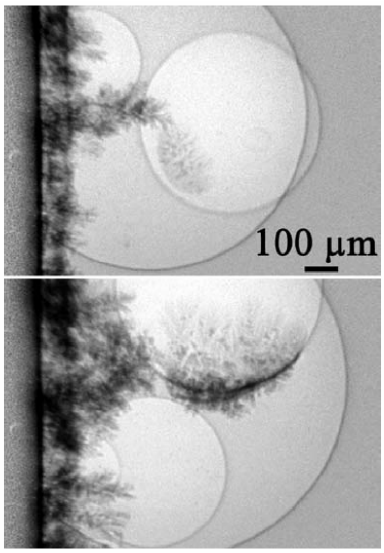

Synchrotron X-ray beams can induce solution precipitation of nanoparticles [35]. By irradiating the aqueous solution of a Ni salt and a reducing agent with synchrotron X-rays, Ni-P alloy homogeneously nucleated in the aqueous solution, eventually growing to nanoparticles [35]. Borse et al. showed that the room temperature formation of magnetic Ni nanoparticles could be possible by X-ray irradiation of alkaline electroless solution [36]. Such studies suggested that synchrotron X-rays could induce solution precipitation of nanoparticles and its application to other metals of alloys could lead to a new method to fabricate nanostructured materials.

Most recently, localised electrochemical deposition (LECD) was studied using microradiography with coherent synchrotron hard X-rays [46,47]. For the first time, the

electrochemical deposition mechanism was revealed by in-situ, real-time observation of the process. LECD is a novel and interesting technique for the fabrication of very high-aspect-ratio microstructures and nanostructures. Figure 9 shows an example of LECD growth of a high-aspect-ratio copper microstructure deposited on a copper substrate at 4.5 V, which was monitored with real-time microradiology with coherent X-rays. In Figure 9(a), the procedure of fabrication of dense microstructure using 'no-contact' mode is shown. The electrode-structure distance was kept constant at 40 μm (upper critical distance). The FESEM analysis of the change in the morphology is demonstrated in Figure 9(b). LECD is less expensive and can be applied to various materials such as metals, metal alloys, conducting polymers, and semiconductors in micrometer, submicrometer, and nanoscale [46,47]. It is expected that clear understanding of the deposition mechanism of LECD processes revealed by X-ray imaging will contribute to further improvement of LECD applications to microelectronics, communications, microrobotics, life sciences, microsensors, actuators, and miniature devices in general [46,47].

Figure 9 LECD growth of a high-aspect-ratio Cu microstructure monitored with real-time microradiology with coherent X-rays. (a) The procedure of fabrication of dense microstructure using 'no-contact' mode. The electrode-structure distance was kept constant at 40 μm (upper critical distance) and (b) FESEM analysis of the change in the morphology [46]

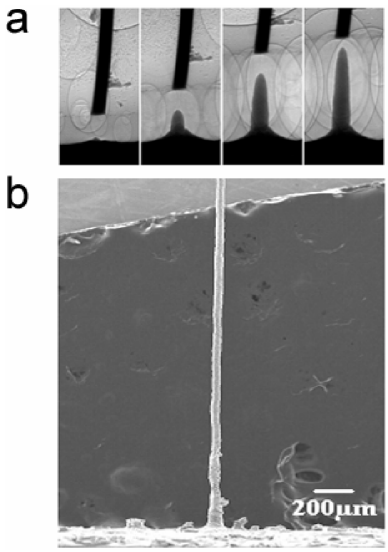

4 Perspectives

The properties of matter at the nanometre scale are dramatically different from the bulk or the constituent molecules. The differences are caused, for example, by quantum confinement, altered thermodynamics, or changed chemical reactivity. In particular, quantum size effects are the most commonly known processes that affect nanostructures. When at least one dimension of a solid sample becomes comparable to the electron de Broglie wavelength, new properties appear. Furthermore, research frontiers in magnetism

concern phenomena at interfaces between nanolayers and those affecting domain nanostructures. Another important area of nanoscience is the small-scale interaction between hard and soft matters, broadly defined to include proteins, lipids, carbohydrates, nucleic acids, and biological molecular systems [40]. High spatial resolution and ultrafast methods to study structures and dynamics of nanomaterials are crucial to the progress in these domains.

It should be noted that progress in synchrotron-like sources is not over yet. So far all high resolution X-ray microscopy experiments were performed at 2nd or 3rd generation electron storage rings [41]. With the forthcoming Free Electron Laser (FEL) X-ray sources and their unique time-structure, increased brilliance and coherence, X-ray imaging techniques will permit time-resolved experiments with even higher energy and spatial resolution [41].

Even without waiting for such futuristic new devices, there is much room for improvements in the techniques described in this review. We are specifically trying to develop the synchrotron hard X-ray imaging based on phase contrast imaging with high lateral resolution to less than 20 nm and high time resolution to 10 μs, which will play a significant role in research on both physical and biological systems at the nanoscales.

Acknowledgements

Our research programs in this domain are supported by KISTEP through the SKORE-A, NRL and STAR Programs, by NCRC (KOSEF) program, by MOCIE, by the National Science Council of Taiwan, by the Swiss Fonds National pour la Recherche Scientifique and by the Ecole Polytechnique Fédérale de Lausanne.

References

1 Röntgen, W.C. (1896) 'On a new kind of rays', *Nature*, Vol. 53, pp.274–276.

2 Webb, A.R. (2003) *Introduction to Biomedical Imaging*, Wiley, New Jersey.

3 Margaritondo, G. (1988) *Introduction to Synchrotron Radiation*, Oxford University Press, Oxford.

4 Margaritondo, G. (2002) *Elements of Synchrotron Radiation for Chemistry, Biology and Medical Research*, Oxford University Press, Oxford.

5 Fitzgerald, R. (2000) 'Phase-sensitive X-ray imaging', *Phys. Today*, Vol. 53, p.23.

6 Raven, C., Snigirev, A., Snigireva, I., Spanne, P., Souvorov, A. and Kohn, V. (1996) 'Phase-contrast microtomography with coherent high-energy synchrotron X-rays', *Appl. Phys. Lett.*, Vol. 69, pp.1826–1828.

7 Arfelli, F., Assante, M., Bonvicini, V., Bravin, A., Cantatore, G., Castelli, E., Dalla Palma, L., Di Michiel, M., Longo, R., Olivo, A., Pani, S., Pontoni, D., Poropat, P., Prest, M., Rashevsky, A., Tromba, G., Vacchi, A., Vallazza, E. and Zanconati, F. (1998) 'Low-dose phase contrast X-ray medical imaging', *Phys. Med. Biol.*, Vol. 43, pp.2845–2852.

8 Bonse, U. and Hart, M. (1965) 'An X-ray interferometer', *Appl. Phys. Lett.*, Vol. 6, pp.155–156.

9 Hart, M. (1971) 'Bragg reflection X-ray optics', *Rep. Prog. Phys.*, Vol. 34, pp.435–490.

10 Momose, A. (1995) 'Demonstration of phase-contrast X-ray computered tomography using an X-ray interferometer', *Nucl. Instrum. Meth. A*, Vol. 352, pp.622–628.

11 Momose, A., Takeda, T., Itai, Y. and Hirano, K. (1996) 'Phase-contrast X-ray computed tomography for observing biological soft tissues', *Nature Med.*, Vol. 2, pp.473–475.

12 Takeda, T., Momose, A., Wu, J., Yu, Q., Zeniya, T., Thet-Thet-Lwin, Yoneyama, A. and Itai, Y. (2002) 'Vessel imaging by interferometric phase-contrast X-ray technique', *Circulation*, Vol. 105, pp.1708–1712.

13 Momose, A. (2003) 'Phase-sensitive imaging and phase tomography using X-ray interferometers', *Opt. Express*, Vol. 11, pp.2303–2314.

14 Ingal, V.N. and Beliaevskaya, E.A. (1995) 'X-ray plane-wave topography observation of the phase contrast from a non-crystalline object', *J. Phys. D: Appl. Phys.*, Vol. 28, pp.2314–2317.

15 Chapman, D., Thomlinson, W., Johnston, R.E., Washburn, D., Pisano, E., Gmür, N., Zhong, Z., Menk, R., Arfelli, F. and Sayers, D. (1997) 'Diffraction enhanced X-ray imaging', *Phys. Med. Biol.*, Vol. 42, pp.2015–2025.

16 Davis, T.J., Gao, D., Gureyev, T.E., Stevenson, A.W. and Wilkins, S.W. (1995) 'Phase-contrast imaging of weakly absorbing materials using hard X-rays', *Nature*, Vol. 373, pp.595–598; Davis, T.J., Gureyev, T.E., Gao, D., Stevenson, A.W. and Wilkins, S.W. (1995) 'X-ray image contrast from a simple phase object', *Phys. Rev. Lett.*, Vol. 74, pp.3173–3175.

17 Wilkins, S.W., Gureyev, T.E., Gao, D., Pogany, A. and Stevenson, A.W. (1996) 'Phase-contrast imaging using polychromatic hard X-rays', *Nature*, Vol. 384, pp.335–338.

18 Pisano, E.D. (2000) 'Current status of full-field digital mammography', *Radiology*, Vol. 214, pp.26–28.

19 Dilmanian, F.A., Zhong, Z., Ren, B., Wu, X.Y., Chapman, L.D., Orion, I. and Thomlinson, W.C. (2000) 'Computed tomography of X-ray index of refraction using the diffraction enhanced imaging method', *Phys. Med. Biol.*, Vol. 45, pp.933–946.

20 Snigirev, A., Snigireva, I., Suvorov, A., Kocsis, M. and Kohn, V. (1995) 'Phase contrast microimaging by coherent high energy synchrotron radiation', *ESRF Newsletter Rep.*, Vol. 24, pp.23–25.

21 Snigirev, A., Snigireva, I., Kohn, V., Kuznetsov, S., and Schelokov, I. (1995) 'On the possibilities of X-ray phase contrast microimaging by coherent high-energy synchrotron radiation', *Rev. Sci. Instrum.*, Vol. 66, pp.5486–5492.

22 Spanne, P., Raven, C., Snigireva, I. and Snigirev, A. (1999) 'In-line holography and phase-contrast microtomography with high energy X-rays', *Phys. Med. Biol.*, Vol. 44, pp.741–749.

23 Arfelli, F., Bonvicini, V., Bravin, A., Cantatore, G., Castelli, E., Dalla Palma, L., Di Michiel, M., Fabrizioli, M., Longo, R., Menk, R. H., Olivo, A., Pani, S., Pontoni, D., Poropat, P., Prest, M., Rashevsky, A., Ratti, M., Rigon, L., Tromba, G., Vacchi, A. and Vallazza, E. (2000) 'Mammography with synchrotron radiation: phase detection techniques', *Radiology*, Vol. 215, pp.286–293.

24 Margaritondo, G. (1998) 'Double take makes the most of X-rays to enhance synchrotron images', *Phys. World*, Vol. 11, pp.28–29.

25 Margaritindo, G. and Tromba, G. (1999) 'Coherence based edge diffraction sharpening of X-ray imaging: a simple model', *J. Appl. Phys.*, Vol. 85, pp.3406–3408.

26 Hwu, Y., Hsieh, H.H., Lu, M.J., Tsai, W.L., Lin, H.M., Lai, B., Je, J.H., Kim, C.K., Noh, D.Y., Youn, H.S., Tromba, G. and Margaritondo, G. (1999) 'Coherence-enhanced synchrotron radiology: refraction versus diffraction mechanisms', *J. Appl. Phys.*, Vol. 86, pp.4613–4618.

27 Hwu, Y., Tsai, W.L., Hsieh, H.H., Je, J.H., Kang, H., Kim, I.W., Lee, K.H., Kim, H.J., Lai, B. and Margaritondo, G. (2001) 'Collimation-enhanced micro-radiography in real-time', *Nucl. Instrum. Meth. A*, Vols. 467–468, pp.1294–1300.

28 Tsai, W.L., Hsu, P.C., Hwu, Y., Chen, C.H., Chang, L.W., Je, J.H., Lin, H.M., Groso, A. and Margaritondo, G. (2002) 'Building on bubbles in metal electrodeposition', *Nature*, Vol. 417, p.139.

29 Hwu, Y., Tsai, W.L., Groso, A., Margaritondo, G. and Je, J.H. (2002) 'Coherence-enhanced synchrotron radiology: simple theory and practical applications', *J. Phys. D: Appl. Phys.*, Vol. 35, pp.R105–R120.

30 Meuli, R., Hwu, Y., Je, J. H. and G. Margaritondo (2004) 'Synchrotron radiation in radiology: radiation techniques used on synchrotron sources', *Eur. J. Radiol.*, Vol. 14, pp.1550–1560.

31 Baik, S., Kim, H.S., Jeong, M.H., Lee, C.S., Je, J.H., Hwu, Y. and Margaritondo, G. (2004) 'International consortium on phase contrast imaging and radiology beamline at the Pohang Light Source', *Rev. Sci. Instr.*, Vol. 75, pp.4355–4358.

32 Hwu, Y., Tsai, W.L., Je, J.H., Seol, S.K., Kim, B., Groso, A., Margaritondo, G., Lee, K-H. and Seoung, J-K. (2004) 'Synchrotron microangiography with no contrast agent', *Phys. Med. Biol.*, Vol. 49, pp.501–508.

33 Hwu, Y., Tsai, W.L., Chang, H.M., Yeh, H.I., Hsu, P.C., Yang, Y.C., Su, Y.T., Tsai, H.L., Chow, G.M. Ho, P.C., Li, S.C., Moser, H.O., Yang, P., Seol, S.K., Kim, C.C., Je, J.H., Stefanekovo, E., Groso, A. and Margaritondo, G. (2004) 'Imaging cells and tissues with refractive index radiology', *Biophys. J.*, Vol. 87, pp.4180–4187.

34 Tsai, W.L., Hwu, Y., Chen, C.H., Chang, L.W., Je, J.H., Lin, H.M. and Margaritondo, G. (2003) 'Grain boundary imaging, gallium diffusion and the fracture behavior of Al-Zn Alloy-An in situ study', *Nucl. Instrum. Meth. B*, Vol. 199, pp.457–463.

35 Lee, H.J., Je, J.H., Hwu, Y. and Tsai, W.L. (2003) 'Synchrotron X-ray induced solution precipitation of nanoparticles', *Nucl. Instrum. Meth. B*, Vol. 199, pp.342–347.

36 Borse, P.H., Yi, J.M., Je, J.H., Choi, S.D., Hwu, Y., Ruterana, P. and Nouet, G. (2004) 'Formation of magnetic Ni nanoparticles in X-ray irradiated electroless (2004) solution', *Nanotechnology*, Vol. 15, pp.S389–S392.

37 Peele, A.G. and Nugent, K.A. (2004) 'Phase measurement using x rays', *Rev. Sci. Instr.*, Vol. 75, pp.3382–3386.

38 Arhatari, B.D., Mancuso, A.P., Peele, A.G. and Nugent, K.A. (2004) 'Phase contrast radiography: image modeling and optimization', *Rev. Sci. Instr.*, Vol. 75, pp.5272–5276.

39 Weissleder, R. (2001) 'Scaling down imaging: molecular mapping of cancer in mice', *Nat. Rev. Cancer*, Vol. 2, pp.1–8.

40 Alberts, B., Bray, D., Johnson, A., Lewis, J., Raff, M., Robert, K. and Walter, P. (2004) *Essential Cell biology*, Garland Science, pp.85–87.

41 Schneider, G. (2003) 'X-ray microscopy: methods and perspectives', *Anal. Bioanal. Chem.*, Vol. 376, pp.558–561.

42 Stampanoni, M., Borchert, G., Abela, R. and Rüegsegger, P. (2003) 'Nanotomography based on double asymmetrical Bragg diffraction', *Appl. Phys. Lett.*, Vol. 82, pp.2922–2924.

43 Pogany, A., Gao, D. and Wilkins, S.W. (1997) 'Contrast and resolution in imaging with a microfocus X-ray source', *Rev. Sci. Instr.*, Vol. 68, pp.2774–2782.

44 Kogoshima, Y., Tsusaka, Y., Yokoyama, K., Takai, K. and Matsui, J. (1999) 'Phase-contrast X-ray imaging using both vertically and horizontally expanded synchrotron radiation X-rays with asymmetric Bragg reflection', *Jpn. J. Appl. Phys.*, Vol. 38, p.L470.

45 Miao, J.W., Ishikawa, T., Johnson, B., Anderson, E.H., Lai, B., and Hodgson, K.O. (2002) 'High resolution 3D X-ray diffraction microscopy', *Phys. Rev. Lett.* Vol. 89, pp.088303.

46 Seol, S.K., Yi, J.M., Jin, X., Kim, C.C., Je, J.H., Tsai, W.L., Hsu, P.C., Hwu, Y., Chen, C.H., Chang, L.W. and Margaritondo, G. (2004) 'Coherent microradiology directly observes a critical cathode-anode distance effect in Localized Electrochemical Deposition', *Electrochem. Solid St.*, Vol. 7, pp.C95–C97.

47 Seol, S.K., Pyun, A.R., Hwu, Y., Margaritondo, G. and Je, J.H. (2005) 'Localized electrochemical deposition of copper monitored using real-time X-ray microradiography', *Adv. Funct. Mater.*, Vol. 15, pp.934–937.